ChemComm

Accepted Manuscript

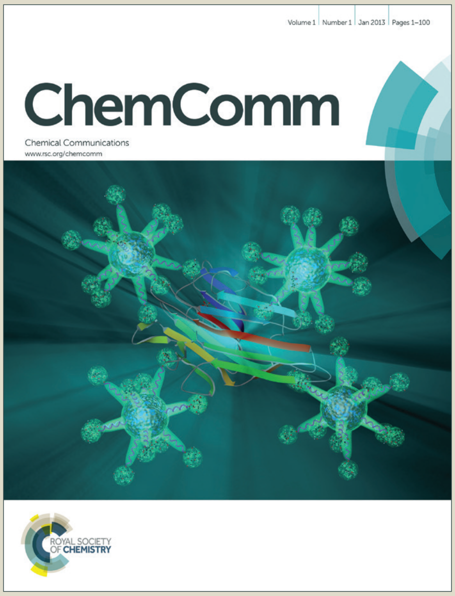

ROYAL SOCIETY OF CHEMISTRY

www.rsc.org/chemcomm

Cite this: DOI: 10.1039/c0xx00000x

www.rsc.org/xxxxxx

Visible light responsive rhodium and antimony-codoped $SrTiO_3$ powdered photocatalyst loaded with IrO_2 cocatalyst for solar water splitting

Rikako Asai,[a] Hiroaki Nemoto,[a] Qingxin Jia,[a] Kenji Saito,[a,‡] Akihide Iwase[a,b] and Akihiko Kudo*[a,b]

Received (in XXX, XXX) Xth XXXXXXXXX 20XX, Accepted Xth XXXXXXXXX 20XX
DOI: 10.1039/b000000x

IrO_2-loaded $SrTiO_3$ doped with rhodium and antimony synthesized by a conventional solid-state reaction split water under visible light and simulated sunlight irradiation giving 0.1% of the apparent quantum yield at 420 nm. The response wavelength up to 500 nm is the longest among achieved photocatalytic water splitting with one-step photoexcitation.

Water splitting using photocatalysts has been extensively studied as a promising candidate for light energy conversion to chemical energy.[1–6] To achieve efficient solar water splitting, it is necessary to develop efficient photocatalysts for one-step or two-step (Z-scheme) water splitting under visible light irradiation.[3,6] Although metal oxides have been known as a useful material group for photocatalytic water splitting,[1–4] developing visible-light-active metal oxide photocatalysts is still challenging.

A photocatalyst for one-step water splitting has to possess thermodynamically satisfied conduction and valence bands for reduction and oxidation of water to H_2 and O_2, respectively. Moreover, a narrow band gap is required for response to visible light. Oxynitride photocatalysts such as GaN-ZnO[7] and $ZnGeN_2$-ZnO[8] solid solutions are well-established materials for water splitting under visible light irradiation. The visible light response of the oxynitride is due to the shallow valence band formed by N2p orbitals. In contrast, the valence band of a metal oxide photocatalyst usually consists of O 2p orbitals (approximately 3.0 V vs. NHE at pH0).[3] The band gap inevitably becomes wider than 3.0 eV, when a conduction band of a metal oxide has an enough high potential for water reduction (0V vs. NHE at pH0). Therefore, many metal oxide photocatalysts show activities for water splitting only under UV light.[1–4]

In order to sensitize metal oxide photocatalysts with wide band gaps to visible light, metal ion doping into the photocatalyst has been studied.[9–13] We have found that Rh-doped $SrTiO_3$ efficiently produces H_2 from an aqueous solution containing a sacrificial reagent under visible light irradiation.[13] In most cases, however, doped metal ions work as charge recombination centers, resulting in low or none photocatalytic activity. We have overcome this problem by codoping other metal cations to maintain the charge balance.[11,12] For example, only Cr-doped TiO_2 is inactive as a photocatalyst, while it shows photocatalytic activity in visible light by codoping Sb.[11] Interestingly, the Rh-doped $SrTiO_3$ photocatalyst which is active for only H_2 evolution produces O_2 from water by codoping Sb, when the photocatalyst is prepared by a hydrothermal method.[14,15] In other words, Rh and Sb-codoped $SrTiO_3$ possesses suitable energy structure to split water under visible light irradiation.

In the present study, we investigated cocatalyst, synthesis, and reaction conditions for the Rh and Sb-codoped $SrTiO_3$ photocatalyst prepared by a conventional solid-state reaction in order to realize the ability of water splitting under visible light or simulated sunlight irradiation.

XRD patterns of $SrTiO_3$:Rh(0.5%),Sb(x%) powders synthesized by a solid-state reaction were the same as that of non-doped $SrTiO_3$ (Figure S1). No observation of additional peaks related with Rh and/or Sb species indicated that Rh and Sb ions were doped into the $SrTiO_3$ lattice. Rh and Sb ions were substituted for a Ti^{4+} ion site which is the B site of perovskite structure (ABO_3), judging from the ionic radii (Ti^{4+}: 0.605 Å, Rh^{3+}: 0.665 Å, Rh^{4+}: 0.6 Å, Sb^{3+}: 0.76 Å, Sb^{5+}: 0.6 Å for 6 coordination). However, any peak shifts in XRD were not observed between $SrTiO_3$ and $SrTiO_3$:Rh,Sb. This is probably because the balance of the larger ionic radius of Rh^{3+} and smaller ionic radius of Sb^{5+} than that of Ti^{4+}; the doped Rh and Sb mainly possessed trivalent and pentavalent, respectively, as discussed in the next paragraph. Although no peak shift was observed in XRD, the substitution of Rh^{3+} and Sb^{5+} for a Ti^{4+} ion site is strongly supported by Raman measurement. A new Raman band at around 800 cm^{-1}, that was not observed for non-doped $SrTiO_3$, appeared with doping Rh and Sb (Figure S2A-a and b). It has been reported that the Raman band at around 800 cm^{-1} is generally observed, when another element is substituted for the B-site of perovskite structure (ABO_3).[16] Interestingly, the intensity of the appeared Raman band at around 800 cm^{-1} depended on the wavelength (532 nm and 785 nm) of the excitation laser (Figure S2); Excitation by 532 nm gave higher intensity than that by 785 nm. This was due to a resonance Raman effect at 532 nm. $SrTiO_3$:Rh,Sb can absorb the light at 532 nm accompanied with the excitation relating doped Rh. Therefore, the resonance Raman effect indicates the doped Rh ions are located at a Ti^{4+} site of $SrTiO_3$. On the basis of XRD and Raman measurements, we can conclude that Rh and Sb ions were doped into a Ti^{4+} ion site of $SrTiO_3$, being similar to the $SrTiO_3$:Rh,Sb synthesized by a hydrothermal method[14,15] and TiO_2:Rh,Sb by a solid-state reaction.[17] The full-width at half maximum (FWHM) of XRD

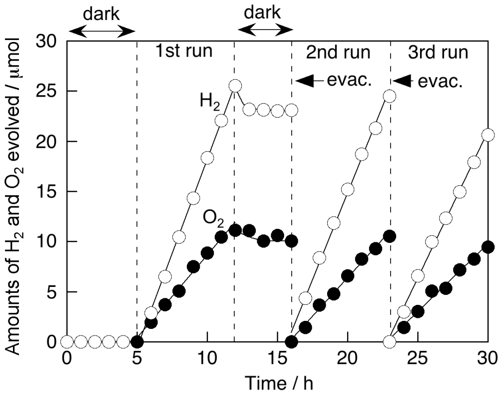

Figure 1. Photocatalytic water splitting over IrO_2(3.0 wt%)-loaded $SrTiO_3$:Rh(0.5%),Sb(1.0%) under visible light irradiation. Catalyst: 0.2 g, reactant solution: 120 mL of $H_2SO_{4\ aq.}$ (pH 3.0), cell: top-irradiation cell, light source: 300-W Xe lamp with a cutoff filter (λ>440 nm).

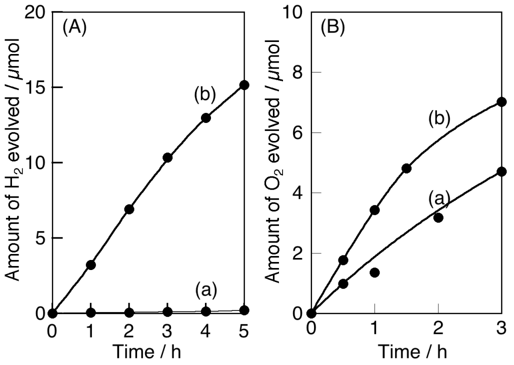

Figure 2. Loading effects of IrO_2 cocatalyst on (A) sacrificial H_2 evolution and (B) O_2 evolution under visible light irradiation over $SrTiO_3$:Rh(0.5%),Sb(1.0%). (a) absence and (b) presence of IrO_2(3 wt%) cocatalyst. Catalyst: 0.2 g, reactant solution: (A) 120 mL of 10vol% MeOH aq., (B) 120 mL of 20 mmol L^{-1} $AgNO_3$ aq., cell: top-irradiation cell, light source: 300-W Xe lamp with a cutoff filter (λ>420 nm).

peak of $SrTiO_3$:Rh,Sb was the same as that of non-doped $SrTiO_3$, indicating that Rh and Sb codoping did not affect the crystallinity of $SrTiO_3$.

Diffuse reflectance spectra of Rh and Sb-codoped $SrTiO_3$ were measured. Although non-doped $SrTiO_3$ had no absorption bands in the visible light range (Figure S3-a), Rh-doped $SrTiO_3$ (Figure S3-b) had two absorption bands at around 420 nm and 580 nm in addition to the band gap absorption of the $SrTiO_3$ host, as previously reported.[13] These two absorption bands have been identified to the Rh^{3+} and Rh^{4+}-related transition by X-ray emission spectroscopy and X-ray absorption spectroscopy.[18] The intensity of the absorptions at around 420 nm and 580 nm increased and decreased, respectively, with increasing the amounts of doped Sb ions (Figure S3-c and d), resulting in the similar profile of the diffuse reflectance spectrum of $SrTiO_3$:Rh,Sb to that of H_2-reduced $SrTiO_3$:Rh (Figure S3-e). This indicates that the amount of Rh ions with lower oxidation number increased by Sb codoping. In other words, the valency of Rh was controlled to trivalent by codoping Sb^{5+} ion to Ti^{4+} ion site, as observed for the hydrothermal-synthesized $SrTiO_3$:Rh,Sb.[14,15] The donor level formed by Rh^{3+} stabilized by Sb-codoping plays an important role for O_2 evolution.[14,15] Rh(0.5%) and Sb(1.0%)-codoped $SrTiO_3$ gave completely different diffuse reflectance spectrum (Figure S3) and photograph (Figure S4) from the mixture of $SrTiO_3$:Rh(0.5%) and $SrTiO_3$:Rh(0.5%),Sb(2.0%) at 1:1 in a molar ratio. This result also indicates that Sb was codoped with Rh in the same particles and contributed to the valency control of doped Rh. As the role of doped Sb^{5+}, not only maintaining the charge balance but also forming a new conduction band as previously reported[4] would be considered. However, the fact that no shift in the band gap absorption between $SrTiO_3$ and $SrTiO_3$:Rh,Sb was observed (Figure S3) indicates that doped Sb^{5+} did not form a new conduction band in the forbidden band of $SrTiO_3$. Moreover, the doped Sb would not affect the position of the conduction band of the $SrTiO_3$ host, because the amount of doped Sb was only 1.0%.

Figure 1 shows water splitting under visible light irradiation over the optimized IrO_2-loaded $SrTiO_3$:Rh,Sb photocatalyst. The highest activity was obtained at pH3 and 3 wt% of the loading amount (Figures S5a and b). The optimum preparation condition of a solid-state reaction was calcined at 1373 K for 10 h (Figure S5c). No H_2 and O_2 evolved in the dark period, indicating that mechano-catalytic water splitting[1,19] did not occur under the current experimental condition. When photocatalyst was irradiated with visible light, water splitting proceeded steadily, resulting in that 71 μmol of H_2 and 31 μmol of O_2 evolved for 21 h. The turnover numbers of the reacted electrons/holes to the amount of IrO_2 cocatalyst and doped Rh were 4.7 and 23, respectively. To check the further potential of this photocatalyst for water splitting under accelerated condition, a 400 W high-pressure lamp was used (Figure S6). The UV light was filtered by an aqueous $NaNO_2$ solution to pass only visible light (λ>400 nm)[7]. The amounts of evolved H_2 and O_2 were 510 μmol and 240 μmol over 21 h, respectively, giving turnover numbers of 14 for IrO_2 cocatalyst and 71 for doped Rh. These results indicate that the water splitting proceeded photocatalytically.

Various cocatalysts were employed for water splitting over $SrTiO_3$:Rh,Sb. Non- and CoO_x-loaded $SrTiO_3$:Rh(0.5%),Sb(1.0%) were inactive for water splitting (Entries 1 and 2 in Table S1). In contrast, $SrTiO_3$:Rh(0.5%),Sb(1.0%) produced H_2 and O_2 from water in a stoichiometric amount under visible light irradiation, when RuO_2, Ru, and IrO_2 were loaded (Entries 3–7 in Table S1). Among them, impregnated IrO_2 was the most effective cocatalyst for water splitting. Non-doped and neither only Rh(0.5%) or Sb(1.0%)-doped $SrTiO_3$ did not show the activity for water splitting even under UV irradiation (Entries 8–10 in Table S1), even if IrO_2 was loaded, being different from $SrTiO_3$:Rh(0.5%),Sb(1.0%).

To clarify whether the IrO_2 cocatalyst enhanced H_2 or O_2 evolution, sacrificial H_2 and O_2 evolutions under visible light irradiation were examined as shown in Figure 2. Non-loaded $SrTiO_3$:Rh,Sb was inactive for sacrificial H_2 evolution, while the activity appeared with loading IrO_2. This appearance of the activity for H_2 evolution clearly indicates that the IrO_2 particle worked as a H_2 evolution site. The activity of $SrTiO_3$:Rh,Sb for O_2 evolution was also improved by loading IrO_2. In the presence of Ag^+ ions, the photogenerated electrons in the $SrTiO_3$:Rh,Sb are consumed by Ag^+ ions because of a large driving force for the reduction of Ag^+. Therefore, the oxidation reaction by holes should be the rate-controlling step in this case; the driving force for the oxidation of water to form O_2 by holes photogenerated in

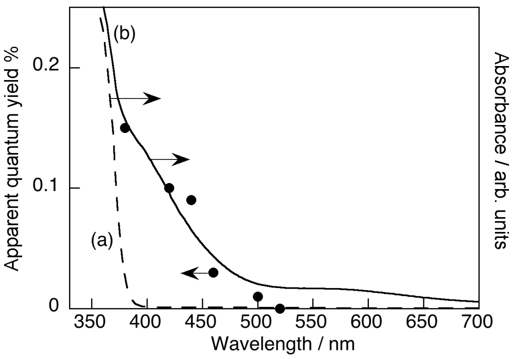

Figure 3. Diffuse reflectance spectra of (a) non-doped $SrTiO_3$ and (b) $SrTiO_3$:Rh(0.5%),Sb(1.0%), and an action spectrum for water splitting over IrO_2(3.0 wt%)/$SrTiO_3$:Rh(0.5%),Sb(1.0%). Catalyst: 0.1 g, reactant solution: 120 mL of H_2SO_4 aq. (pH 3.0), cell: top-irradiation cell.

an impurity level consisting of Rh^{3+} would not be large. Therefore, we can conclude that the improved O_2 evolution activity is due to the improvement for the water oxidation by the loaded IrO_2. Thus, IrO_2 which is a well-known cocatalyst for O_2 evolution[20,21] enhanced not only O_2 evolution but also H_2 evolution in water splitting using $SrTiO_3$:Rh,Sb. The similar enhancement in both reduction and oxidation reactions was observed for RuO_2 cocatalyst.[22] The mechanism of the enhancement in the H_2 evolution by IrO_2 has not been clarified yet, while the possible explanation would be that partially reduced IrO_2 worked as an active site for H_2 evolution. In general, the backward reaction to form H_2O from H_2 and O_2 evolved by water splitting proceeds rapidly on the surface of metallic Ir.[20] However, a decrease in evolved H_2 and O_2 was not observed in the dark period after the 1st run of water splitting as shown in Figure 1, indicating that the backward reaction between H_2 and O_2 to form water was negligible. This result implies that the partially-reduced IrO_2 still remained as an oxide denoted as IrO_x.

In order to clarify that the water splitting is caused by the photoexcitation of $SrTiO_3$:Rh,Sb, an action spectrum for water splitting over IrO_2-loaded $SrTiO_3$:Rh(0.5%),Sb(1.0%) was measured as shown in Figure 3. The onset of the action spectrum agreed well with the edge of an absorption band relating doped Rh^{3+}. Therefore, the agreement of the action spectrum with the diffuse reflectance spectrum of $SrTiO_3$:Rh(0.5%),Sb(1.0%) indicates that water splitting over IrO_2-loaded $SrTiO_3$:Rh(0.5%),Sb(1.0%) proceeded accompanied with the transition from electron donor levels consisting of Rh^{3+} to the conduction band of $SrTiO_3$. The photocatalyst responded to visible light up to 500 nm. This response wavelength was longer than 480 nm for both $(Ga_{1-x}Zn_x)(N_{1-x}O_x)$[7] and $(Zn_{1.44}Ge)(N_{2.08}O_{0.38})$[8] of visible-light-driven photocatalysts for water splitting. The apparent quantum yield was calculated to be 0.1% at 420 nm.

To indicate the possibility of the solar water splitting for practical use, IrO_2/$SrTiO_3$:Rh,Sb was also irradiated with simulated sunlight. IrO_2/$SrTiO_3$:Rh,Sb split water into H_2 and O_2 steadily in a stoichiometric amount under simulated sunlight irradiation (Figure S7). When 1 m^2 of the irradiated area was assumed, the rates of H_2 and O_2 evolution were 26 mL h^{-1} and 13 mL h^{-1}, respectively, giving 0.01% of solar energy conversion efficiency.

Conclusions

In conclusion, Rh and Sb were homogeneously codoped into the $SrTiO_3$ crystal lattice by a simple solid-state reaction. IrO_2-loaded $SrTiO_3$:Rh,Sb photocatalyst of a one-step photoexcitation system split water under visible light irradiation. We successfully achieved water splitting under visible light irradiation using a metal oxide photocatalyst with well-controlled band structure. This photocatalyst responded to visible light up to 500 nm. This response wavelength is the longest among previously reported photocatalysts for water splitting with one-step photoexcitation system. Thus, the doping of metals to provide visible light response and the codoping to control the valency of the doped metals will be a new and effective strategy to develop visible-light-driven metal oxide photocatalysts for overall water splitting.

Notes and references

[a] *Department of Applied Chemistry, Faculty of Science, Tokyo University of Science, 1-3 Kagurazaka, Shinjyuku-ku, Tokyo 162-8601, JAPAN, Tel: +81-3-5228-8267; E-mail: a-kudo@rs.kagu.tus.ac.jp*

[b] *Photocatalyst International Research Center, Research Institute of Science and Technology, Tokyo University of Science, JAPAN*

† Electronic Supplementary Information (ESI) available: [Experimental details, characterization, optimization]. See DOI: 10.1039/b000000x/

‡ Office for Development of Young Researchers, Research Planning and Promotion Division, Niigata University, 8050 Ikarashi 2-no-cho, Nishi-ku, Niigata 950-2181, JAPAN

1 K. Domen, J. N. Kondo, M. Hara, T. Takata, *Bull. Chem. Soc. Jpn.* 2000, **73,** 1307.
2 F. E. Osterloh, *Chem. Mater.* 2008, **20,** 35.
3 A. Kudo, Y. Miseki, *Chem. Soc. Rev.* 2009, **38,** 253.
4 Y. Inoue, *Energy Environ. Sci.* 2009, **2,** 364.
5 K. Maeda, K. Domen, *J. Phys. Chem. Lett.* 2010, **1,** 2655.
6 R. Abe, *J. Photochem. Photobiol. C* 2010, **11,** 179.
7 K. Maeda, K. Teramura, T. Takata, M. Hara, N. Saito, K. Toda, Y. Inoue, H. Kobayashi, K. Domen, *J. Phys. Chem. B* 2005, **109**, 20504.
8 Y. Lee, H. Terashima, Y. Shimodaira, K. Teramura, M. Hara, H. Kobayashi, K. Domen, *J. Phys. Chem. C* 2007, **111,** 1042.
9 M. Matsumura, M. Hiramoto, H. Tsubomura, *J. Electrochem. Soc.* 1983, **130,** 326.
10 H. P. Maruska, A. K. Ghosh, *Sol. Energy. Mater.* 1979, **1**, 237.
11 H. Kato, A. Kudo, *J. Phys. Chem. B* 2002, **106**, 5029.
12 T. Ishii, H. Kato, A. Kudo, *J. Photochem. Photobiol. A* 2004, **163**, 181.
13 R. Konta, T. Ishii, H. Kato, A. Kudo, *J. Phys. Chem. B* 2004, **108**, 8992.
14 K. Furuhashi, Q. Jia, A. Kudo, H. Onishi, *J. Phys Chem. C* 2013, **117**, 19101.
15 R. Niishiro, S. Tanaka, A. Kudo,. *Appl. Cat. B: Environ.*, 10.1016/j.apcatb.2013.12.015.
16 H. Zheng, I. M. Reaney, G. D. C. Csete de Györgyfalva, R. Ubic, J. Yarwood, M. P. Seabara, V. M. Ferreira, *J. Mater. Res.* 2004, **19**, 488.
17 R. Niishiro, R. Konta, H. Kato, W. J. Chun, K. Asakura, A. Kudo, *J. Phys. Chem. C* 2007, **111**, 17420.
18 S. Kawasaki, K. Akagi, K. Nakatsuji, S. Yamamoto, I. Matsuda, Y. Harada, J. Yoshinobu, F. Komori, R. Takahashi, M. Lippmaa, C. Sakai, H. Niwa, M. Oshima, K. Iwashina, A. Kudo, *J. Phys. Chem. C* 2012, **116**, 24445.
19 S. Ikeda, T. Takata, T. Kondo, G. Hitoki, M. Hara, J. N. Kondo, K. Domen, H. Hosono, H. Kawazoe, A. Tanaka, *Chem. Commun.* 1998, 2185.
20 A. Iwase, H. Kato, A. Kudo, *Chem. Lett.* 2005, **34**, 946.
21 M. Hara, C. C. Waraksa, J. T. Lean, B. A. Lewis, T. E. Mallouk, *J. Phys. Chem. A* 2000, **104**, 5275.
22 K. Maeda, R. Abe, K. Domen, *J. Phys. Chem. C* 2011, **115**, 3057.